Stochastic diffusion processes on Cartesian meshes

Lina Meinecke[1], Per Lötstedt[1]

[1] *Division of Scientific Computing, Department of Information Technology*
Uppsala University, P. O. Box 337, SE-75105 Uppsala, Sweden
email: lina.meinecke@it.uu.se, perl@it.uu.se

Abstract

Diffusion of molecules is simulated stochastically by letting them jump between voxels in a Cartesian mesh. The jump coefficients are first derived using finite difference, finite element, and finite volume approximations of the Laplacian on the mesh. An alternative is to let the first exit time for a molecule in random walk in a voxel define the jump coefficient. Such coefficients have the advantage of always being non-negative. These four different ways of obtaining the diffusion propensities are compared theoretically and in numerical experiments.

Keywords. stochastic simulation, diffusion, Cartesian mesh

AMS subject classification. 65C05, 65C35, 92C05, 92C42

1 Introduction

Small copy numbers of many molecular species in biological cells require stochastic models of the chemical reactions between the molecules and their diffusive motion. One example is gene expression where the number of molecules involved is small and only stochastic models can explain observations in experiments [5, 20]. Continuum models for the concentrations of the chemical species based on partial differential equations (PDEs) capture neither the randomness in the chemical reactions nor the fact that the number of molecules is integer.

In a well stirred system, there is no space dependence of the distribution of the species. Gillespie [9] invented an algorithm to simulate such chemical systems, the Stochastic Simulation Algorithm (SSA). The efficiency of the algorithm is improved in [8]. It is extended in [4, 11] to space-dependent systems where the diffusion of the molecules cannot be neglected. Space is partitioned by a Cartesian mesh into compartments or voxels $\mathcal{V}_i$ with a node $\mathbf{x}_i$ in the center in [4] and the molecules jump between the voxels (or between the nodes in the lattice) with a certain probability. The time until a molecule jumps from $\mathcal{V}_i$ to the adjacent $\mathcal{V}_j$ is assumed to be exponentially distributed with parameter λ_{ij}. With n_i neighbours, the total jump propensity out of $\mathcal{V}_i$ is

$$\lambda_i = \sum_{j=1}^{n_i} \lambda_{ij}. \tag{1}$$

The diffusion propensity is $\lambda_i m_i$ with m_i molecules in $\mathcal{V}_i$. Then the SSA for the diffusion in the molecular system is:

1. Initialize the number of molecules $m_k, k = 1, \ldots, K$, in the K voxels at $t = 0$.

2. Sample the exponentially distributed time Δt_k with rate $\lambda_k m_k$ to the first diffusion event in all K voxels and let $t_k = \Delta t_k$.

3. Determine the smallest t_k. Let t_i be the minimum in voxel $\mathcal{V}_i$.

4. For the jump from $\mathcal{V}_i$, sample a jump to $\mathcal{V}_j$ with probability $\theta_{ij} = \lambda_{ij}/\lambda_i$.

5. Update $t := t_i$, m_i and m_j.

6. Sample Δt_i and Δt_j with rates $\lambda_i m_i$ and $\lambda_j m_j$ and let $t_i = t + \Delta t_i$ and $t_j = t + \Delta t_j$ and go to 3.

We will compare different ways of determining non-negative jump coefficients λ_{ij} for a Cartesian mesh in this paper.

The coefficients λ_{ij} are first chosen by approximating the Laplacian of u on a mesh with a node at $\mathbf{x}_i$

$$\Delta u \approx \sum_{j=1}^{n_i} \lambda_{ij} u_j - \lambda_i u_i = \sum_{j=1}^{n_i} \lambda_{ij}(u_j - u_i), \tag{2}$$

where u_j is the numerical solution at a surrounding node $\mathbf{x}_j$. In an equidistant Cartesian mesh the Laplacian is discretized with a finite difference method (FDM), in [4, 7, 11]. The coefficients for an unstructured mesh are derived from a finite element method (FEM) for the Laplacian in [3, 6] and with a finite volume method (FVM) in [12]. The justification for this choice is that as the number of molecules M grows, the time-dependent expected values of the concentrations of the molecules converge to the solution of the diffusion equation discretized in space [15].

The jump propensities λ_{ij} have to be non-negative to be meaningful in the SSA. The standard 5-point (2D) and 7-point (3D) approximations of the Laplace operator with FDM on a Cartesian mesh yield positive λ_{ij} for the neighbouring voxels but the FEM coefficients for an unstructured mesh may be negative for a poor mesh. The numerical discretization of the Poisson equation by a common FVM method may be inconsistent and not converge to the analytical solution on a general unstructured mesh but the coefficients are non-negative.

If the jump coefficients are negative, the numerical solution of the diffusion equation or the Poisson equation will in general not be monotone and not satisfy the discrete maximum principle. For the discrete maximum principle to hold the coefficients must satisfy the following conditions, see [2]: (1) is valid for interior nodes; $\lambda_{ij} \geq 0$; and λ_i is greater than the sum of the off-diagonal elements for at least one boundary node. Thus, the two first conditions apply for both the diffusion coefficients in the SSA and the discretization of the diffusion equation.

Many papers are devoted to the derivation of consistent FEM and FVM approximations fulfilling the discrete maximum principle for triangular and quadrilateral meshes in 2D and tetrahedral meshes in 3D, e.g. [1, 13, 16, 22, 23]. They are nonlinear and depend on the solution making them less suitable as jump propensities in the SSA or rely on meshes with geometrical properties that may be difficult to achieve with a mesh generator. In [14, 17] it has been shown that it is impossible to construct a linear method for a linear elliptic equation on general quadrilateral meshes in 2D satisfying the discrete maximum principle.

As an alternative, we compute the diffusion coefficients in the SSA from the distribution for the first exit time (FET) τ from the voxels for a molecule in Brownian motion. The mesh is Cartesian in 2D with different mesh sizes h_x and h_y in the x and y directions, respectively. The expected value of the FET from $\mathcal{V}_i$ is the inverse of the rate λ_i. The probability to exit to $\mathcal{V}_j$ depends on the distance between the nodes $\mathbf{x}_i$ and $\mathbf{x}_j$ i.e. h_x and h_y. These coefficients are always non-negative. They are compared with the methods above for approximations of the Laplacian.

In the next section, we present the coefficients for FDM, FEM, and FVM. We compute the FET in Sect. 3. In Sect. 4, we compare the four methods to obtain λ_i and θ_{ij}. We perform numerical experiments in Sect. 5 and draw conclusions in the final section.

2 FDM, FEM, and FVM coefficients

The mesh we consider is Cartesian in 2D with nodes $\mathbf{x}_i$ and a dual mesh with voxels $\mathcal{V}_i$ with $\mathbf{x}_i$ in the center. The distance is h_x between the nodes in the x direction and h_y in the y direction. In the following, we consider the reference voxel $\mathcal{V}_0$ with midpoint $\mathbf{x}_0$ and area $h_x h_y$, see Fig. 1, and introduce the aspect ratio κ, such that $h_x = \kappa h$ and $h_y = h$.

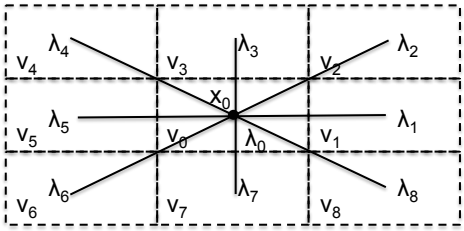

Fig. 1: The reference nine point stencil in 2D for the voxel $\mathcal{V}_0$ with midpoint $\mathbf{x}_0$ and its neighbours.

2.1 FDM

Discretize the Laplacian Δ with the FDM to obtain the weights λ_i in the difference stencil for the mesh in Fig. 1. By symmetry, $\lambda_1 = \lambda_5, \lambda_3 = \lambda_7$, and $\lambda_2 = \lambda_4 = \lambda_6 = \lambda_8$ and by consistency, the weight in the center point is $-\sum_{j=1}^{8} \lambda_j$. The following coefficients obtained after Taylor expansion give a second order approximation of Δ

$$\lambda_1 = \frac{1-\kappa\alpha}{\kappa^2 h^2},\ \lambda_2 = \frac{\alpha}{2\kappa h^2},\ \lambda_3 = \frac{\kappa^2 - \kappa\alpha}{\kappa^2 h^2}, \tag{3}$$

where α is a free parameter. If $\alpha = 0$ then we have the usual 5-point stencil. We wish all λ_i to be non-negative to fulfill the discrete maximum principle and to be useful as jump coefficients requiring

$$0 \le \alpha \le \min\left(\kappa, \frac{1}{\kappa}\right) \le 1. \tag{4}$$

The weight in the center is

$$\lambda_0 = 2\frac{\kappa^2 - \alpha\kappa + 1}{\kappa^2 h^2} > 0 \tag{5}$$

with a negative sign. As $\kappa \to \infty$, $\alpha \to 0$ for positive coefficients and $\lambda_0 \to 2/h_y^2$. For a large κ, almost all jumps out of $\mathcal{V}_0$ will be in the y direction with the same rate as in 1D. Accordingly, if $\kappa \to 0$, then $\alpha \to 0$ and $\lambda_0 \to 2/h_x^2$ and the diffusion behaves as one-dimensional in the x direction. The jump rate to node i is λ_i and the relative rates $\theta_i = \lambda_i/\lambda_0$ between the nodes in Sect. 1 are

$$\theta_1 = \theta_5 = \frac{1-\alpha\kappa}{2(\kappa^2 - \alpha\kappa + 1)},\ \theta_3 = \theta_7 = \frac{\kappa^2 - \alpha\kappa}{2(\kappa^2 - \alpha\kappa + 1)},$$
$$\theta_2 = \theta_4 = \theta_6 = \theta_8 = \frac{\alpha\kappa}{4(\kappa^2 - \alpha\kappa + 1)}. \tag{6}$$

With $\alpha = 0$ and $\kappa = 1$, the non-zero relative rates are $\theta_1 = \theta_3 = \theta_5 = \theta_7 = 1/4$, the 5-point stencil.

2.2 FEM

We approximate the Laplacian by bilinear basis functions on a rectangular element as in [2]. The lumped mass matrix has $h_x h_y$ on the diagonal. After division by $h_x h_y$, the coefficients corresponding to λ_i in (3) and (5) are

$$\lambda_0 = \frac{4(\kappa^2+1)}{3\kappa^2 h^2},\ \lambda_1 = \frac{2-\kappa^2}{3\kappa^2 h^2},\ \lambda_2 = \frac{\kappa^2+1}{6\kappa^2 h^2},\ \lambda_3 = \frac{2\kappa^2-1}{3\kappa^2 h^2}. \tag{7}$$

The free parameter α in (3) is here $(\kappa^2+1)/(3\kappa)$ with the following constraints on the mesh for non-negative the coefficients

$$\frac{1}{\sqrt{2}} \le \kappa \le \sqrt{2}. \tag{8}$$

The relative rates are

$$\theta_1 = \theta_5 = \frac{2-\kappa^2}{4(\kappa^2+1)},\ \theta_3 = \theta_7 = \frac{2\kappa^2-1}{4(\kappa^2+1)},\ \theta_2 = \theta_4 = \theta_6 = \theta_8 = \frac{1}{8}, \tag{9}$$

cf. (6).

2.3 FVM

The Laplacian in the FVM is approxiated by:

$$\Delta u(\mathbf{x}_0) \approx \frac{1}{|\mathcal{V}_0|}\int_{\mathcal{V}_0} \Delta u\, d\Omega = \frac{1}{|\mathcal{V}_0|}\int_{\nu_0} \mathbf{n}\cdot\nabla u\, ds = \frac{1}{|\mathcal{V}_0|}\sum_{j=1}^{4}\int_{\nu_{0j}} \mathbf{n}\cdot\nabla u\, ds \tag{10}$$

in voxel $\mathcal{V}_0$ of area $|\mathcal{V}_0| = h_x h_y = \kappa h^2$ and with normal $\mathbf{n}$ at the boundary $\nu_0 = \bigcup_{j=1}^{4}\nu_{0j}$. We now approximate the outward fluxes $\mathbf{n}\cdot\nabla u$ across the edges. Suppose that u_j is the solution in $\mathcal{V}_j, j = 1,\ldots,8$, surrounding $\mathcal{V}_0$ in Fig. 1 and u_0 is the solution in $\mathcal{V}_0$. The straightforward approximation of the outward flux on the edge ν_{01} in (10) is $(u_1 - u_0)/h_x$. Similar approximations on the other edges yield the coefficients

$$\lambda_0 = \frac{2(\kappa^2+1)}{\kappa^2 h^2},\ \lambda_1 = \frac{1}{\kappa^2 h^2},\ \lambda_2 = 0,\ \lambda_3 = \frac{1}{h^2}, \tag{11}$$

corresponding to the case $\alpha = 0$ in (3). There is no problem with negative jump propensities here. The relative rates in the SSA in Sect. 1 are

$$\theta_1 = \theta_5 = \frac{1}{2(\kappa^2+1)},\ \theta_3 = \theta_7 = \frac{\kappa^2}{2(\kappa^2+1)},\ \theta_2 = \theta_4 = \theta_6 = \theta_8 = 0. \tag{12}$$

In another gradient approximation involving the diagonal voxels, let $\partial u/\partial x \approx (u_1 + u_2 - (u_0 + u_3))/2h_x$ in the corner to $\mathcal{V}_2$, see Fig. 1. With the same kind of approximation for $\partial u/\partial y$ and in the other corners of $\mathcal{V}_0$ and a linear variation of the gradient along ν_{0j}, the coefficients are

$$\lambda_1 = \lambda_5 = \frac{1-\kappa^2}{2\kappa^2 h^2},\ \lambda_2 = \lambda_4 = \lambda_6 = \lambda_8 = \frac{1+\kappa^2}{4\kappa^2 h^2},\ \lambda_3 = \lambda_7 = \frac{\kappa^2-1}{2\kappa^2 h^2},\ \lambda_0 = 4\lambda_2. \tag{13}$$

These are non-negative only if $\kappa = 1$. Then they are the same as for the FDM with $\alpha = 1$ in Sect. 2.1.

3 First exit time

Let the first exit time (FET) of a molecule initially at $\mathbf{x}_0$ from a domain ω with boundary $\partial\omega$ be denoted by the random variable τ. The mean value $E_\tau = E[\tau]$ and the location on $\partial\omega$ where the molecule left ω can be computed from the probability density for the position of the molecule. Let $c(\mathbf{x}, t)$ satisfy the following PDE with diffusion coefficient D in ω:

$$\frac{\partial c(\mathbf{x},t)}{\partial t} = D\Delta c(\mathbf{x},t),\ \mathbf{x}\in\omega, \quad c(\mathbf{x},t) = 0,\ \mathbf{x}\in\partial\omega, \quad c(\mathbf{x},0) = \delta(\mathbf{x}-\mathbf{x}_0). \tag{14}$$

Then $c(\mathbf{x}, t)$ is the probability density for the position $\mathbf{x}$ of a diffusing molecule provided that it has not left ω until time t [10, 18, 19, 21]. The probability that the molecule is still inside ω at t is the survival probability

$$S(t) = \int_\omega c(\mathbf{x},t)\,d\omega = P(\tau \geq t). \tag{15}$$

Let $\mathbf{n}$ denote the outward normal of $\partial\omega$. The probability density function (PDF) for a molecule to exit at time t is then derived from (14) and Gauss' formula

$$p_\omega(t) = -\frac{\partial S(t)}{\partial t} = -\int_\omega D\Delta c\,d\omega = -D\int_{\partial\omega} \mathbf{n}\cdot\nabla c\,ds \geq 0. \tag{16}$$

The expected value is obtained from $p_\omega(t)$

$$E_\tau = \int_0^\infty t p_\omega(t)\,dt = \int_0^\infty S(t)\,dt. \tag{17}$$

Since $S(0) = 1$, $\lim_{t\to\infty} S(t) = 0$, and $S(t)$ decays monotonically it is well approximated by an exponential $S(t) \approx \tilde{S}(t) = \exp(-\lambda t)$. With this $\tilde{S}$, by (17) $E_\tau = 1/\lambda$ and by (16) the approximate PDF of the exit time τ is

$$\tilde{p}_\omega(t) = \lambda\exp(-\lambda t). \tag{18}$$

i.e. τ is exponentially distributed. The diffusion propensity λ_0 in the SSA in Sect. 1 to jump out of $\mathcal{V}_0$ is then $1/E_\tau$ with the corresponding domain ω_0 surrounding $\mathcal{V}_0$, see Fig. 2a.

The flux of molecules out of ω_0 at a point on $\partial\omega_0$ is $-D\nabla c\cdot\mathbf{n}$. Let $\partial\omega_0$ consist of non-overlapping sections $\partial\omega_j$ such that $\partial\omega_0 = \bigcup_j \partial\omega_j$. The probability that the molecule leaves ω_0 at $\partial\omega_j$ of the boundary is

$$p_{\partial\omega_j}(t) = -D\int_{\partial\omega_j} \mathbf{n}\cdot\nabla c(\mathbf{x},t)\,ds \tag{19}$$

Given that the exit time out of a neighbourhood ω_0 is t, the conditional probability for the molecule to exit along the edge $\partial\omega_j$ is

$$\theta_j(t) = \frac{p_{\partial\omega_j}(t)}{p_{\partial\omega_0}(t)} = \frac{\int_{\partial\omega_j}\mathbf{n}\cdot\nabla c(\mathbf{x},t)\,ds}{\int_{\partial\omega_0}\mathbf{n}\cdot\nabla c(\mathbf{x},t)ds}. \tag{20}$$

The probability in the SSA to leave ω_0 through $\partial\omega_j$ at time τ is then the expected value

$$\theta_j = E[\theta_j(\tau)] = \int_0^\infty \theta_j(t)p_\omega(t)\,dt \tag{21}$$

and by (20) $\sum_j \theta_j = 1$. No matter how we choose ω_0, the θ_j are always non-negative.

To calculate the coefficients for the voxel in Fig. 1 we choose ω_0 to be the rectangle defined by the surrounding nodes $\mathbf{x}_1, \ldots, \mathbf{x}_8$, see Fig. 2a. We compute the jump rate λ_0 by (15) and (17). The boundary $\partial\omega_0$ is partitioned into $\partial\omega_j, j = 1, \ldots, 8$, centered around the nodes $\mathbf{x}_j$. We choose two parameters $0 \leq \beta_x, \beta_y \leq 1$ such that $|\partial\omega_1| = |\partial\omega_5| = 2\beta_y h_y$ and $|\partial\omega_3| = |\partial\omega_7| = 2\beta_x h_x$, where $|\cdot|$ is the length of an edge. Consequently, the length of $\partial\omega_2$, $\partial\omega_4$, $\partial\omega_6$, and $\partial\omega_8$ is $(1-\beta_x)h_x + (1-\beta_y)h_y$. Then θ_j follows from (20) and (21).

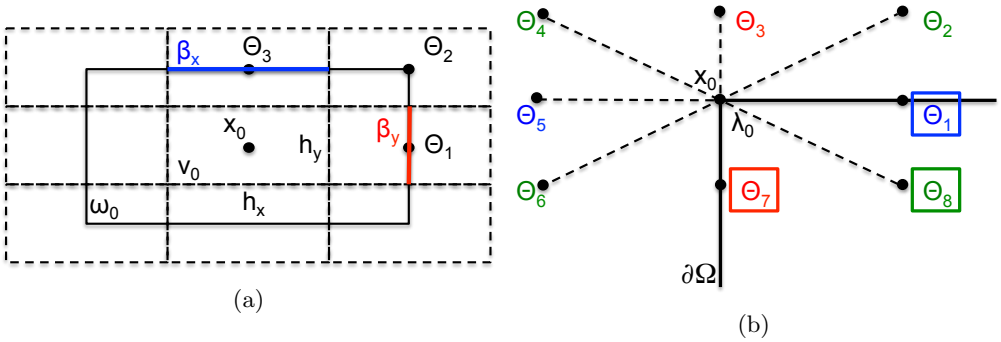

Fig. 2: (a) The voxel $\mathcal{V}_0$ embedded in the rectangle ω_0. (b) Boundary treatment for a corner.

The analytical solution of (14) with $\mathbf{x}_0 = (h_x, h_y)$ in the rectangular domain $\omega = [0, 2h_x] \times [0, 2h_y]$ is obtained by an expansion in the eigenfunctions

$$\begin{aligned} c(x,y,t) &= \sum_{k=1}^{\infty}\sum_{j=1}^{\infty} \frac{1}{h_x h_y} \sin\left(\frac{k\pi}{2}\right) \sin\left(\frac{j\pi}{2}\right) \sin\left(\frac{k\pi x}{2h_x}\right) \sin\left(\frac{j\pi y}{2h_y}\right) \cdot \\ &\quad \cdot \exp\left(-\left(\frac{k^2}{4h_x^2} + \frac{j^2}{4h_y^2}\right)\pi^2 D t\right) \qquad (22) \\ &= \frac{1}{\kappa h^2} \sum_{k=1}^{\infty}\sum_{j=1}^{\infty} (-1)^{j+k} \sin\left(\frac{(2k-1)\pi x}{2\kappa h}\right) \sin\left(\frac{(2j-1)\pi y}{2h}\right) \cdot \\ &\quad \cdot \exp\left(-\frac{\pi^2 D t}{4\kappa^2 h^2}\left((2j-1)^2 + \kappa^2(2k-1)^2\right)\right). \end{aligned}$$

Choosing $\beta_x = \beta_y = 1$ corresponds to $\alpha = 0$ in the FDM in Sect. 2.1. In that case, jumps only happen along the coordinate axes of the mesh and coordinate splitting allows us to simulate two one dimensional diffusions instead. The choice $\beta_x = \beta_y = 0$ corresponds to $\alpha = 1$ in Sect. 2.1 with only the nodes in the corners involved.

By (15), (17) and (23) the jump rate from $\mathbf{x}_0$ out of ω_0 is

$$\frac{1}{\lambda_0} = \frac{64\kappa^2 h^2}{\pi^4 D} \sum_{j=1}^{\infty}\sum_{k=1}^{\infty} \frac{(-1)^{j+k}}{(2j-1)(2k-1)\left((2j-1)^2 + \kappa^2(2k-1)^2\right)}. \qquad (23)$$

There are two parameters in the definition of the FET coefficients, β_x and β_y. They determine $\partial\omega_j$ and θ_j in (20) and (21). At the edge where $x = 2\kappa h$, $p_{\partial\omega_1}$ is given by (19)

$$\begin{aligned} p_{\partial\omega_1}(t, \beta_y, \kappa) &= \int_{(1-\beta_y)h}^{(1+\beta_y)h} \frac{\partial c}{\partial x}\, dy \\ &= \frac{2}{\kappa^2 h^2} \sum_{k=1}^{\infty}\sum_{j=1}^{\infty} (-1)^{k+1} \frac{2k-1}{2j-1} \sin\left(\frac{(2j-1)\pi\beta_y}{2}\right) \cdot \exp\left(-\frac{\pi^2 D t}{4\kappa^2 h^2}\left((2j-1) + \kappa^2(2k-1)^2\right)\right). \end{aligned}$$

(24)

Hence, θ_1 in (21) depends nonlinearly on β_y and κ, and accordingly for θ_3 and β_x.

Henceforth, the diffusion coefficient D is taken to be 1. Examples of time dependent solutions to (15) and (20) are found in Fig. 3 for $\kappa = 1.4$ and $h = 1$. The survival probability $S(t)$ is well approximated in Fig. 3a by an exponential except for small t.

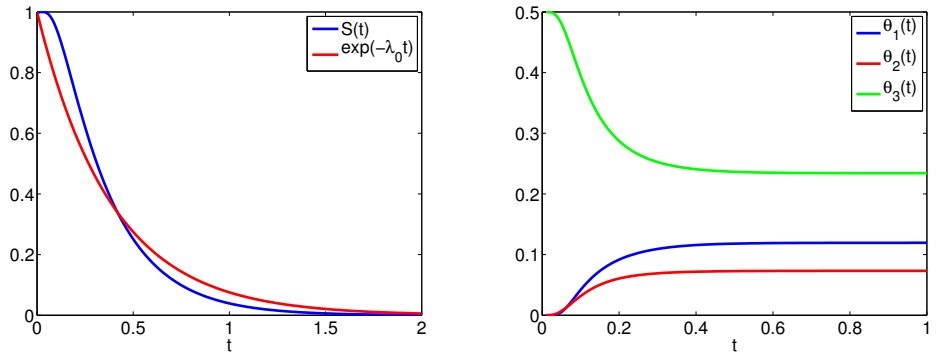

(a) (b)

Fig. 3: FET quantities calculated for $\kappa = 1.4$, $h = 1$, $D = 1$ and $\beta_x = \beta_y = 0.5$: (a) $S(t)$ and approximation by an exponential. (b) $\theta_j(t)$.

The jump coefficients θ_j are computed for a $t > 0$ in Fig. 3b. A finite summation of the solution in (24) is oscillatory for small t due to the slow convergence of the series. For small t and $\kappa > 1$ jumps are more likely to occur in the y direction, i.e. to $\mathbf{x}_3$ and $\mathbf{x}_7$ since $\theta_3 > \theta_1, \theta_2$. When t is large, it follows from (24) that the sums are well approximated by their first term, $c_j \exp(-\gamma t)$, where $\gamma = \pi^2 D(1+\kappa^2)/4\kappa^2 h^2$, resulting in

$$\theta_j \approx \frac{c_j \exp(-\gamma t)}{\sum_{k=1}^{8} c_k \exp(-\gamma t)} = \frac{c_j}{\sum_{k=1}^{8} c_k}, \tag{25}$$

the constant behaviour for large times we see in Fig. 3b.

4 Comparison of the coefficients

The FEM, FVM, and FET define the coefficient λ_0 without any parameter. We can then choose the free parameter α such that the FDM coefficient corresponds to either of them:

$$\alpha_{FEM} = \frac{1+\kappa^2}{3\kappa},\ \alpha_{FVM} = 0,\ \alpha_{FET} = \frac{\kappa^2\left(1-\frac{1}{2}\lambda_0 h^2\right)+1}{\kappa}, \tag{26}$$

The values of λ_0 and α for $\kappa = 1$ and $\kappa = 1.4$ are found in Table 1.

		FEM	FVM	FET
$\kappa = 1$	$\lambda_0 \cdot h^2$	2.6667	4	3.3934
	α	0.6667	0	0.3033
$\kappa = 1.4$	$\lambda_0 \cdot h^2$	2.0136	3.0204	2.5841
	α	0.7048	0	0.3054

Table 1: The jump coefficients for different methods when $\kappa = 1$ and $\kappa = 1.4$ and α is such that the FDM has the same λ_0.

By choosing α as in (26) we obtain the same relative jump coefficients θ_j as the FEM (9) and the FVM (12). The relative jump coefficients in FET depend on β_x and β_y in Sect. 3. By solving

$$\theta_{1,FET}(\beta_y) = \theta_{1,FDM}, \quad \theta_{3,FET}(\beta_x) = \theta_{3,FDM}, \tag{27}$$

numerically for β_x and β_y and using that by symmetry

$$\theta_{5,FET} = \theta_{1,FET},\ \theta_{3,FET} = \theta_{7,FET},\ \theta_{j,FET} = (1 - 2\theta_{1,FET} - 2\theta_{3,FET})/4,\ j = 2, 4, 6, 8,$$

the FET jump coefficients agree with those from FDM. With $\kappa = 1.4$, the values of β_x and β_y are 0.511 and 0.7381, respectively. With this choice of β_x and β_y, the FET coefficients define a second order approximation of the Laplacian. In Fig. 4, we see the behaviour of $\beta_x, \beta_y, \lambda_0$ and the appropriate α for different κ. As κ increases, $\lambda_0 h^2 \to 2$ converging again to the one-dimensional case, compare also (23). In Fig. 4b, we find that an increase in κ affects β_y - regulating the contribution from the shorter edge - more than β_x, which only slightly depends on κ.

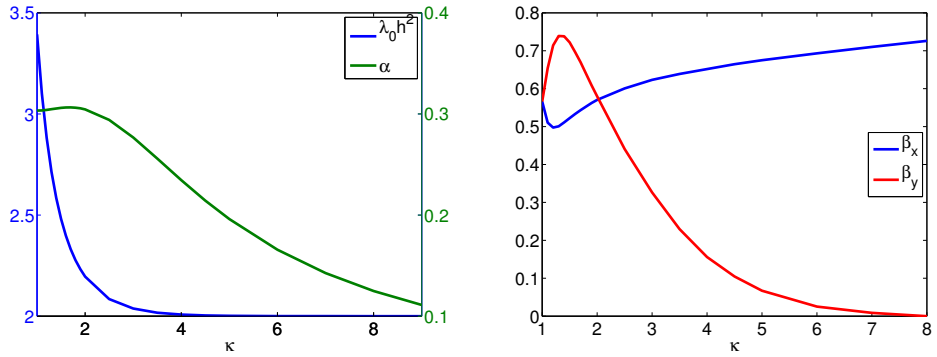

(a) (b)

Fig. 4: (a) The α parameter (right) in FDM to achieve the same $h^2\lambda_0$ as in FET in (26) and the corresponding $\lambda_0 h^2$. (b) The β coefficients in FET in (27) to achieve the same relative jump coefficients θ_j for the same λ_0 as in FDM.

5 Numerical results

We will now examine the performance of the coefficients in SSA simulations of the diffusion of molecules. A square $\Omega = [0, 20] \times [0, 20]$ is discretized in the experiments into n_x nodes or grid

points in the x-direction and $n_y = \kappa(n_x - 1) + 1$ in the y-direction. The boundary is defined by the first and the last nodes in the x and y directions. We choose $\kappa = 1$ and $\kappa = 1.4$. The molecules are reflected as they reach the boundary. The distribution of molecules is compared to the analytical solution of the diffusion equation with Neumann boundary conditions:

$$\frac{\partial u(\mathbf{x},t)}{\partial t} = \Delta u(\mathbf{x},t),\ \mathbf{x} \in \Omega, \quad \frac{\partial u}{\partial n} = 0,\ \mathbf{x} \in \partial\Omega, \quad u(\mathbf{x},0) = \delta(\mathbf{x} - \mathbf{x}_0). \tag{28}$$

To implement the reflecting boundary condition we add the contributions θ_j from the standard voxel at the boundary, which are outside the domain, to θ_j in the interior, see Fig. 2b.

Let M be the number of molecules and the final time $T = 5$. The molecules are released at $t = 0$ at the center $\mathbf{x}_0 = (10, 10)$ of the domain. The error e in the simulations is defined by

$$e^2 = \sum_{i=1}^{n_x} \sum_{j=1}^{n_y} |\mathcal{V}_{ij}| \left| \frac{m_{ij}}{M\kappa h^2} - u(\mathbf{x}_{ij}, T) \right|^2, \tag{29}$$

where m_{ij} is the copy number in voxel (i, j), $|\mathcal{V}_{ij}|$ is the volume of voxel $\mathcal{V}_{ij}$ and $\mathbf{x}_{ij}$ is the node coordinate. As the FDM, the FEM, and the FVM are second order accurate, their errors will behave as $\mathcal{O}(h^2 + M^{-\frac{1}{2}})$ because of the space discretization and the statistical error.

In the case $\kappa = 1$, we have $\beta_x = \beta_y = \beta$. The β value is chosen such that $\theta_{i,FET} = \theta_{i,FDM}$ with $\alpha = 0.3033$. The relative jump coefficients vary with β in Fig. 5a. At $\beta \approx 0.56$ they agree with the FDM coefficients in (6), see also Fig. 4b. We calculate the error on a grid with $n_x = n_y = 21$ grid points and $M = 5 \cdot 10^6$ and see that the accuracy varies with β in Fig. 5b. The minimum is at $\beta \approx 0.56$ where the FET is equal to an FDM in Fig. 5a and is second order accurate.

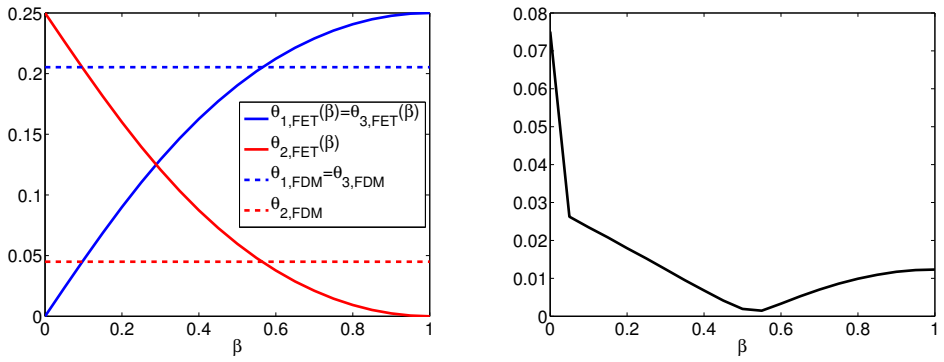

(a) (b)

Fig. 5: Comparison between FDM with $\alpha = \alpha_{FET}$ and FET at $\kappa = 1$: (a) Relative jump propensities depending on parameter β in FET and the constant FDM coefficients. (b) Error e for different values of β.

The FET jump coefficients for different $\beta = \beta_x = \beta_y$ are compared to FDM coefficients for $\kappa = 1.4$ in Fig. 6a. The error for the same parameters as before is displayed in Fig. 6b with a minimum at $\beta \approx 0.5$. The isolines of the error for combinations of β_x and β_y are found in Fig. 6c.

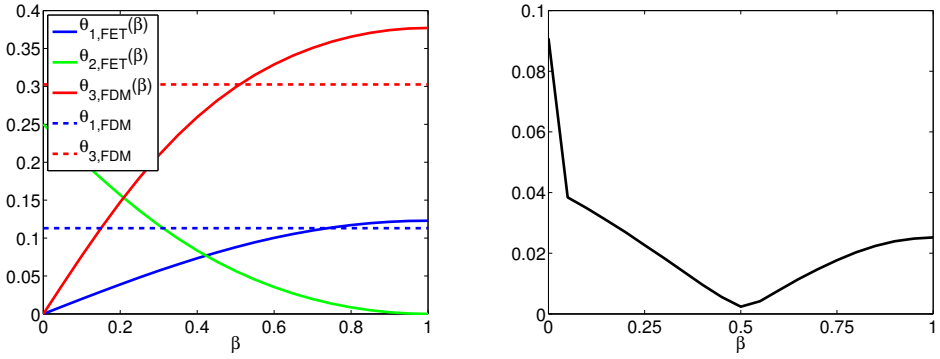

(a)

(b)

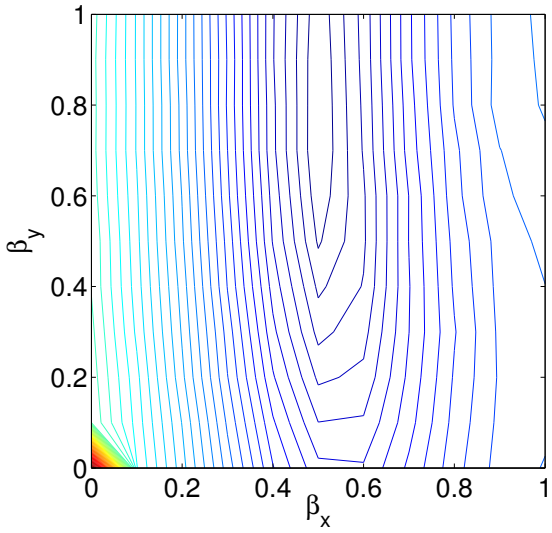

(c)

Fig. 6: Comparison between FDM with $\alpha = \alpha_{FET}$ and FET at $\kappa = 1.4$: (a) Relative jump propensities for FET depending on parameter β and the constant FDM coefficients. (b) Error for different values of $\beta = \beta_x = \beta_y$. (c) Level curves of the error for different values of β_x and β_y.

We observe in Fig. 6a that the match with the FDM coefficients occurs for $\beta_x = 0.511$ and $\beta_y = 0.738$, which coincides with the minimum in Fig. 6c. The FET viewed as an approximation to the Laplacian is second order accurate there. The simplification $\beta = \beta_x = \beta_y$ has its minimum at $\beta \approx 0.5$ in Fig. 6b. This value corresponds to integration in (24) and in Fig. 2a between the boundaries of the adjacent voxels $\mathcal{V}_1, \mathcal{V}_2$, and $\mathcal{V}_3$ to obtain θ_1, θ_2, and θ_3, respectively.

In Fig. 5b and Figs. 6b,c, the error increases suddenly when β and β_x and β_y approach 0, which corresponds to $\alpha = 1$ in the FDM. Then the molecules only jump along the diagonals, which means - if they are released in one voxel - they cover the domain in a checkerboard pattern. This unnatural diffusion explains the high error.

We measure the relative error $e/\|u\|$ in Fig. 7a for the four different methods where e is

calculated as in (29) and

$$\|u\|^2 = \sum_{i=1}^{n_x} \sum_{j=1}^{n_y} |\mathcal{V}_{ij}||u(x_{ij}, T)|^2. \tag{30}$$

We discretize the square into $n_x = 11, 21$ and 41 nodes and choose $\kappa = 1.4$, such that $n_y = 15, 29$ and 57 and $\kappa h = 2, 1$ and 0.5. We set $M = 10n_x^4$ in order to keep the statistical error smaller than the spatial error. In Fig. 7b, we display the error in the FDM for $\alpha \leq 1/\kappa$, where $\kappa = 1.4$, $M = 5 \cdot 10^6$ and $n = 21$. The error increases slightly with increasing α and the fluctuations indicate the size of the statistical error. Furthermore, we count the number of jumps for each simulation. This number is proportional to the number of generated random numbers and the administration of an event in the system - and therefore the computational work - and we plot the error against it in Fig. 7c.

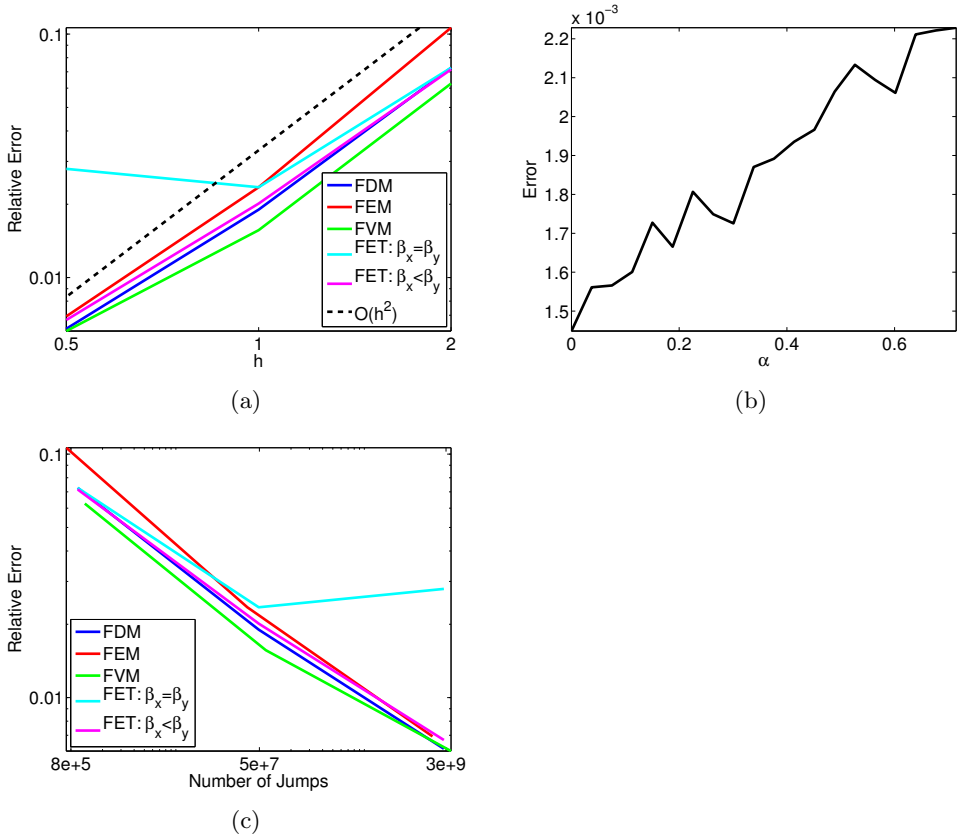

Fig. 7: Performance on a square domain with $\kappa = 1.4$ (a) Convergence for the FDM with $\alpha = 0.3054$, the FVM, the FEM, and the FET with $\beta_x = \beta_y = 0.5$ and $\beta_x = 0.511$ and $\beta_y = 0.738$. The reference curve decays as h^2. (b) Error for the FDM method for different parameters α. (c) Relative error versus the number of jumps needed in each simulation.

The three methods FDM, FVM, and FEM converge to the analytical solution of the diffusion equation with rate 2 in Fig. 7a, as expected. There is a unique choice of β_x and β_y such that the FET corresponds to the FDM and becomes second order, too. With $\beta_x = \beta_y = 0.5$, the FET is not a consistent approximation of Δ and no reduction in $e/\|u\|$ is observed when h is

lowered from 1 to 0.5. The relative error stagnates at $0.02 - 0.03$ which is sufficiently low for most problems. The minimum error for the FDM is obtained for $\alpha = 0$ in Fig. 7b. This method is the standard five point approximation and is equal to the FVM in (11) and (12). In Table 1, the FEM has the smallest λ_0. As the exit time is distributed exponentially, that means that the FEM has the longest expected time between events, corresponding to fewer jumps being simulated in $[0, T]$. For a given error, the number of jumps should be as low as possible for the best efficiency. As the FEM corresponds to a FDM with $\alpha = 0.7048$ it generates a higher error. The FET or the FDM with $\alpha = 0.3054$ on the other hand result in a smaller error while still jumping less than the FVM or the FDM with $\alpha = 0$. In the comparison in Fig. 7c, the difference between the methods is small.

6 Conclusions and discussion

We evaluate four different ways of computing jump coefficients between voxels for stochastic simulation of diffusion in a Cartesian mesh; as a distinctive feature we include jumps along the diagonals in the mesh. The method based on the first exit time (FET) is equivalent to a finite difference method (FDM) of second order accuracy if the parameters are chosen appropriately. The most accurate method compared to the solution of the diffusion equation on a square is to use the coefficients of the finite volume method (FVM) or equivalently a FDM without including the diagonals. If we count the number of jumps to obtain a certain relative error, the differences between the methods are minor. The FVM and FET coefficients are always non-negative. There are restrictions on the mesh for the finite element method (FEM) to generate non-negative coefficients and for a given mesh there are restrictions on the FDM for non-negativity.

A generalization of these methods to an unstructured mesh consisting of triangles as in [6] is desirable for improved geometrical flexibility. The straightforward FVM in Sect. 2.3 is easily adapted to a triangulated domain. A FEM with linear basis and test functions will generate jump coefficients as in [6]. A FDM consistent with the Laplacian is not easily derived analytically. However, the FVM may not be consistent and the jump coefficients of the FEM may be negative. The FET is easily transformed to an unstructured mesh. The analytical solution of (14) is no longer possible but $c(\mathbf{x}, t), \lambda_0$, and θ_j can be computed numerically. The jump coefficients are non-negative but there is no FDM to help us determine β. Taking $\beta = 0.5$ works fairly well in Sect. 5 for reasonable error levels. The inconsistency with the Laplacian plays a role only for very small errors in the numerical experiments. Hence, this would be the natural choice for an unstructured mesh. The generalization to triangular meshes of the calculation of the diffusion jump coefficients will be the subject of a forthcoming paper.

References

[1] E. Burman and A. Ern. Stabilized Galerkin approximation of convection-diffusion-reaction equations: Discrete maximum principle and convergence. *Math. Comp.*, 74:1637–1652, 2005.

[2] I. Christie and C. Hall. The maximum principle for bilinear elements. *Int. J. Numer. Meth. Eng.*, 20:549–553, 1984.

[3] B. Drawert, S. Engblom, and A. Hellander. URDME: a modular framework for stochastic simulation of reaction-transport processes in complex geometries. *BMC Syst. Biol.*, 6:76, 2012.

[4] J. Elf and M. Ehrenberg. Spontaneous separation of bi-stable biochemical systems into spatial domains of opposite phases. *Syst. Biol.*, 1:230–236, 2004.

[5] M. B. Elowitz, A. J. Levine, E. D. Siggia, and P. S. Swain. Stochastic gene expression in a single cell. *Science*, 297(5584):1183–1186, 2002.

[6] S. Engblom, L. Ferm, A. Hellander, and P. Lötstedt. Simulation of stochastic reaction-diffusion processes on unstructured meshes. *SIAM J. Sci. Comput.*, 31:1774–1797, 2009.

[7] C. W. Gardiner, K. J. McNeil, D. F. Walls, and I. S. Matheson. Correlations in stochastic theories of chemical reactions. *J. Stat. Phys.*, 14(4):307–331, 1976.

[8] M. A. Gibson and J. Bruck. Efficient exact stochastic simulation of chemical systems with many species and many channels. *J. Phys. Chem.*, 104(9):1876–1889, 2000.

[9] D. T. Gillespie. A general method for numerically simulating the stochastic time evolution of coupled chemical reactions. *J. Comput. Phys.*, 22(4):403–434, 1976.

[10] D. T. Gillespie and E. Seitaridou. *Simple Brownian Diffusion.* Oxford University Press, Oxford, 2013.

[11] J. Hattne, D. Fange, and J. Elf. Stochastic reaction-diffusion simulation with MesoRD. *Bioinformatics*, 21:2923–2924, 2005.

[12] I. Hepburn, W. Chen, S. Wils, and E. De Schutter. STEPS: efficient simulation of stochastic reaction-diffusion models in realistic morphologies. *BMC Syst. Biol.*, 6:36, 2012.

[13] R. Horváth. Sufficient conditions of the discrete maximum-minimum principle for parabolic problems on rectangular meshes. *Comp. Math. Appl.*, 55:2306–2317, 2008.

[14] E. Keilegavlen, J. M. Nordbotten, and I. Aavatsmark. Sufficient criteria are necessary for monotone control volume methods. *Appl. Math. Lett.*, 22:1178–1180, 2009.

[15] T. G. Kurtz. Solutions of ordinary differential equations as limits of pure jump Markov processes. *J. Appl. Prob.*, 7:49–58, 1970.

[16] K. Lipnikov, D. Svyatskiy, and Y. Vassilevski. A monotone finite volume scheme for advection-diffusion equations on unstructured polygonal meshes. *J. Comput. Phys.*, 229:4017–4032, 2010.

[17] J. M. Nordbotten, I. Aavatsmark, and G. T. Eigestad. Monotonicity conditions for control volume methods. *Numer. Math.*, 106:255–288, 2007.

[18] B. Øksendal. *Stochastic Differential Equations.* Springer, Berlin, 6th edition, 2003.

[19] T. Opplestrup, V. V. Bulatov, G. H. Gilmer, M. H. Kalos, and B. Sadigh. First-passage Monte Carlo algorithm: diffusion without all the hops. *Phys. Rev. Lett.*, 97:230602, 2006.

[20] A. Raj and A. van Oudenaarden. Nature, nurture, or chance: Stochastic gene expression and its consequences. *Cell*, 135(2):216–226, 2008.

[21] S. Redner. *A Guide to First-Passage Processes.* Cambridge University Press, Cambridge, 2001.

[22] Z. Sheng and G. Yuan. An improved monotone finite volume scheme for diffusion equation on polygonal meshes. *J. Comput. Phys.*, 231:3739–3754, 2012.

[23] V. Thomée and L. Wahlbin. On the existence of maximum principles in parabolic finite element equations. *Math. Comp.*, 77:11–19, 2008.